



Universiteit
Leiden
The Netherlands

Preclinical validation of putative targets in cardiovascular and metabolic disease

Nahon, J.E.

Citation

Nahon, J. E. (2018, November 15). *Preclinical validation of putative targets in cardiovascular and metabolic disease*. Retrieved from <https://hdl.handle.net/1887/66799>

Version: Not Applicable (or Unknown)

License: [Licence agreement concerning inclusion of doctoral thesis in the Institutional Repository of the University of Leiden](#)

Downloaded from: <https://hdl.handle.net/1887/66799>

Note: To cite this publication please use the final published version (if applicable).

Cover Page



Universiteit Leiden



The handle <http://hdl.handle.net/1887/66799> holds various files of this Leiden University dissertation.

Author: Nahon, J.E.

Title: Preclinical validation of putative targets in cardiovascular and metabolic disease

Issue Date: 2018-11-15



Universiteit
Leiden

<http://hdl.handle.net/###>

Hematopoietic Stabilin-1 deficiency does not influence atherosclerosis susceptibility in low-density lipoprotein receptor knockout mice

Joya E. Nahon, Menno Hoekstra, Silvia van Hulst,
Calin Manta, Sergij Goerdts, Janine J. Geerling,
Cyrill Géraud and Miranda Van Eck

ABSTRACT

Background and aims. Stabilin-1 (Stab-1) is a scavenger receptor expressed on alternatively activated macrophages and sinusoidal endothelial cells. Its ligands include oxidized low-density lipoprotein (LDL) and the extracellular matrix glycoprotein SPARC and it is present in both human and murine atherosclerotic lesions. We aimed to investigate the effect of specific deletion of Stab-1 in bone marrow-derived cells, including macrophages on atherosclerotic lesion formation in mice.

Methods. Either wild-type (WT) or Stab-1 knockout (KO) bone marrow was transplanted into LDL receptor KO (LDLr KO) mice after ablation of the endogenous bone marrow by irradiation. The transplanted mice were fed a Western-type diet for 9 weeks to induce atherosclerotic lesion formation.

Results. Interestingly, LDLr KO mice reconstituted with Stab-1 KO bone marrow showed increased body weight gain (two-way ANOVA, $p < 0.001$) and larger white adipocyte cell size (43% increase in cell area, $p < 0.05$) as compared to WT transplanted mice, which correlated positively ($r = 0.82$, $p < 0.001$). Despite these changes, no differences in serum lipids, in vivo foam cell formation or circulating leukocytes were observed. Moreover, atherosclerotic lesion size or composition was not different between both experimental groups.

Conclusion. Bone marrow-specific Stabilin-1 deletion does not affect the susceptibility for atherosclerosis in mice. However, the increased body weight gain and adipocyte cell size highlights a potential role for Stab-1 in metabolic disorders.

INTRODUCTION

Scavenger receptors are a group of structurally diverse surface receptors denominated by their ability to recognize a great variety in ligands (reviewed in: Van Berkel et al. [1]). These ligands include pathogens, apoptotic cells and modified (e.g. oxidized, glycosylated) lipoproteins. Stabilin-1 (Stab-1, FEEL-1, CLEVER-1, MS-1) is a class H scavenger receptor. Stab-1 was originally identified by Goerdts and colleagues as MS-1, a scavenger receptor on liver sinusoidal endothelial cells that mediates the uptake of oxidized low-density lipoproteins (oxLDL) [2,3]. In addition to oxLDL, the extracellular matrix glycoprotein secreted protein acidic and rich in cysteine (SPARC) [3,4], advanced glycosylation end products, pathogens and apoptotic cells are recognized by Stab-1, defining it as a true scavenger receptor [5–7]. Besides executing its classical scavenger function in liver sinusoidal endothelial cells, Stab-1 on lymphatic endothelial cells facilitates T-lymphocyte transmigration and modulates the angiogenic capacity of human umbilical vein endothelial cells [8,9]. In addition to endothelial cells, Stab-1 is expressed in subsets of (tissue) macrophages both under physiological and inflammatory conditions [10,11]. The expression of Stab-1 can be upregulated in macrophages by stimulation with interleukin-4 (IL-4) and dexamethasone and is downregulated upon stimulation with interferon-gamma (INF- γ) [12]. Interestingly, Stab-1 expression is induced both in human atheroma samples as well as in an apolipoprotein E knockout (ApoE KO) murine model for atherosclerosis, as shown by a combination of tissue microarrays and quantitative immunohistochemistry [13]. In the atheroma samples, Stab-1 is expressed both in endothelial cells and in macrophage-rich areas. Furthermore, monocytes, macrophage precursors, circulating in patients with familiar hypercholesterolemia show an increased surface expression of Stab-1 [14] and monocyte Stab-1 has been shown to have an immune modulatory function [15]. Importantly, Stab-1 is highly expressed on M2 macrophages, and M2 macrophages display an increased susceptibility to macrophage foam cell formation [16,17]. Based on these combined findings, it can be hypothesized that macrophage Stab-1 may play a role in the development of atherosclerotic lesions. In the current study we therefore investigated the impact of bone marrow Stab-1 deficiency on the atherogenic process.

MATERIAL AND METHODS

Experimental animals

C57BL/6 and low-density lipoprotein receptor knockout (LDLr KO) mice (The Jackson Laboratory, Bar Harbor, ME) were bred in house at the animal facility of the Leiden Academic Centre for Drug Research. Male C57BL/6J and Stab-1 KO donor mice on a C57BL/6J background were bred in house at the Medical Faculty Mannheim of the Ruprecht-Karls University of Heidelberg and maintained at the animal facility of the Leiden Academic Centre

for Drug Research until the start of the experiment. The experiment was executed in rooms that were temperature controlled and had a 12h/12h light dark cycle. The mice were kept in sterilized filter-top cages for the duration of the experiment. All animal work was approved by the Dutch Ethics Committee and regulatory authority at Leiden University and was carried out in compliance with Dutch government guidelines and the Directive 2010/63/EU of the European Parliament on the protection of animals used for scientific purposes and complies with the ARRIVE guidelines.

Stabilin-1 expression under atherogenic conditions

Peritoneal macrophages (PM) were elicited by injecting 1 mL 3% Brewer's thioglycollate medium (Difco, Detroit, MI) into the peritoneal cavity of C57BL/6 mice. Five days after injection, cells were harvested by PBS lavage of the peritoneal cavity. To generate bone marrow-derived macrophages (BMDM), bone marrow cells were isolated from femurs of C57BL/6 mice and cultured for 7 days in complete RPMI medium supplemented with 20% FCS and 30% L929 cell-conditioned medium as a source of macrophage colony-stimulating factor. After harvesting, PM and BMDM were cultured overnight in DMEM containing 10% FCS. Subsequently, cells were loaded with 20 ng/mL oxLDL for 48 hours in DMEM containing 0.2% BSA to generate foam cells. A RNeasy mini kit (Qiagen, Chatsworth, CA) was used to isolate total RNA (N=3 per group). After checking the concentration and integrity of the RNA and an amplification step (Ambion, #IL1791), the MouseWG-6 v2.0 microarray was performed according to manufacturer's specifications (Illumina, San Diego, CA).

For the analysis of the expression of Stab-1 in the developing lesions, data was used from a microarray dataset acquired by our group as published in Ackers-Johnson et al. 2015 [18]. In short, bilateral collars were placed around carotid arteries in male LDLr KO mice fed a Western-type diet containing 0.25% cholesterol and 0.15% cacao butter (SDS, Sussex, UK) to induce localized atherosclerotic lesion development [19]. RNA was isolated from snap-frozen, pooled carotid arteries that were harvested every two weeks from week 0 to week 10 after induction of atherosclerotic lesion formation. Microarray analysis was performed after processing of the RNA using the Illumina Bead-Chip Whole Genome Microarray platform (ServiceXS). In an independent experiment, these conditions were replicated and RNA was isolated for validation using RT-PCR.

Bone marrow transplantation

The bone marrow recipient male LDLr KO mice were randomized into two groups according to equal age, weight and total and free cholesterol levels and irradiated with two consecutive doses of 4.5 Gy (0.141 Gy/min, 200 kV, 4 mA) using an Andrex Smart 225 Röntgen source (XYLON International, Copenhagen, Denmark) with a 6-mm aluminum filter one day before the bone marrow transplantation. Mice either received bone marrow from C57BL/6J mice (WT) (N=12) or Stab-1 KO mice on a C57BL/6J background (N=11). Hereto, femurs and tibia

were flushed over a 70- μ m cell strainer (Greiner Bio-One, Alphen a/d Rijn, The Netherlands) with PBS to obtain bone marrow in a single cell suspension. 5×10^6 bone marrow cells were injected intravenously into the tail vein of the irradiated mice. The bone marrow transplanted mice were left to recover for nine weeks, during which they received sterilized regular chow diet (Special Diet Services, Witham, Essex, UK). Subsequently, the mice were switched to a Western-type diet (WTD) containing 15% cocoa butter and 0.25% cholesterol (Special Diet Services, Witham, Essex, UK) to induce the development of atherosclerotic lesions. At nine weeks after the start of WTD, the mice were anesthetized by a mix of xylazine (70 mg/kg), ketamine (350 mg/kg) and atropine (1.8 mg/kg). Blood was collected via the orbital sinus and peritoneal cells were isolated, after which the mice were perfused with PBS. Heart, spleen, bone marrow and gonadal white adipose tissue were collected. Genomic DNA was isolated from bone marrow using a PureLink[®] Genomic DNA Mini Kit (Life Technologies, Bleiswijk, The Netherlands). PCR analysis was performed on this genomic DNA using Stab-1 primers (Eurogentec S.A., Seraing, Belgium) to confirm hematological chimerism of the transplanted animals (Figure 1, Table 1).

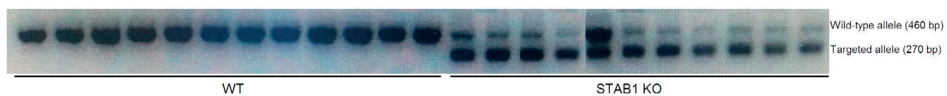


Figure 1. Successful disruption of Stab-1 in bone marrow after transplantation. PCR on genomic DNA isolated from bone marrow of WT (N=12) and Stab-1 KO (N=11) bone marrow transplanted mice at 18 weeks after transplantation.

Table 1. Nucleotide sequence of Stab-1 primers used for PCR.

Primer	Specifications	Nucleotide sequence
mStab1_pcr_A1F	Forward	AGACTATGGTCTCAGTCTGGGA
mStab1_pcr_B461Rwt	Reverse, WT specific	CTGCAATCACGTGCCACACT
mStab1_pcr_C1224R	Reverse	TTATTTCATACCCGCCAGTTCTGA

Histological analysis

The hearts were fixed for 72 hours in 3.7% neutral-buffered formalin (Shandon Formal-Fixx, Thermo scientific, Runcorn, UK) and stored in 0.1% sodiumazide in PBS. Prior to sectioning, hearts were embedded in Tissue-Tek[®] O.C.T. TM (Sakura Finetek, Alphen a/d Rijn, The Netherlands) for 24 hours. Sections of the aortic root were generated using a CM3050S cryostat (Leica, Rijswijk, The Netherlands) at 10 μ m intervals and collected serially. Neutral lipids were stained using Oil Red O (Sigma-Aldrich, Zwijndrecht, The Netherlands). Hematoxylin (Sigma-Aldrich) was used to stain nuclei. Masson's Trichrome staining (Sigma-Aldrich) was used to determine collagen content. For the macrophage staining, a primary monoclonal Rat-anti-mouse CD68 antibody (FA-11; ab53444; Abcam, Cambridge, UK) was used after 1:1000 dilution in block buffer. A secondary AP-conjugated goat-anti-rat IgG (A8438, Sigma-Aldrich,

Zwijndrecht, The Netherlands) was used at a dilution of 1:100 in block buffer. For detection, the ready-to-use BCIP[®]/NBT liquid substrate system was used (Sigma-Aldrich, Zwijndrecht, The Netherlands). Mean lesion area (μm^2) was quantified with a Leica DMRE microscope and HC PL FLUOTAR objective, coupled to a video camera using Qwin V3 software (Leica Ltd, Cambridge, UK). Lesion area and collagen content were quantified blinded and started at tricuspid valves in four lipid and collagen stained sections. White adipose tissue was embedded in paraffin and sectioned using a RM2235 rotary microtome (Leica) at intervals of 5 μm . Sections were stained with hematoxylin and eosin (Merck, Darmstadt, Germany). Adipocyte cell area was quantified using a Leica DMRE microscope and HC PL FLUOTAR objective, coupled to a video camera using Qwin V3 software (Leica Ltd, Cambridge, UK), at magnification 10 \times . Qwin V3 software was used to measure the total area of the image. Subsequently, adipocyte cells were manually counted within this area and the adipocyte cell area was determined by dividing the total area by the number of adipocytes counted. Quantification consisted of 3 sections per mouse. Quantification was performed blinded.

Plasma lipids

Plasma concentrations of total cholesterol, free cholesterol and triglycerides were determined using enzymatic colorimetric assays as described by Out et al (Roche Diagnostics, Mannheim, Germany) [20]. The cholesterol distribution over the different lipoproteins was determined per group by fractionation of 30 μL of pooled plasma using a Superose 6 column (3.2 \times 300 mm, Smart-system, Pharmacia, Uppsala, Sweden) to perform fast protein liquid chromatography (FPLC).

Hematological analysis

An hematological analysis was performed on blood and peritoneal cells using an XT-2000i Automated Hematology Analyzer (Sysmex Corporation, Etten-Leur, The Netherlands). The total amount of leukocytes and the percentage of peritoneal foam cells was determined. After lysis of erythrocytes using ACK lysis buffer, leukocyte populations were determined by flow cytometry using a BD FACS Canto II (BD Biosciences, San Jose, CA). FlowJo software (Flowjo, LCC / BD Biosciences, San Jose, CA) was used to determine monocytes (CD11b+Ly6G⁻), neutrophils (CD11b+Ly6G⁺), B-cells (CD19⁺) and T-cells (CD3⁺) (CD11b: BioLegend, San Diego, CA; Ly6G: BD Biosciences, San Jose, CA; CD19 and CD3: ThermoFisher Scientific, Waltham, MA).

RT-PCR

RNA was isolated from peritoneal cells using the guanidium thiocyanate/phenol/chloroform extraction method according to Chomczynski and Sacchi [21] and reverse transcribed by RevertAid Reverse Transcriptase (Life Technologies). Relative gene expression was measured using SYBR Green Technology (Eurogentec, Maastricht, The Netherlands) on an ABI PRISM

7500 Taqman apparatus (Applied Biosystems, Bleiswijk, The Netherlands). Primers were validated for identical efficiencies. Primer sequences can be found in Table 2. Beta-actin (Actb), glyceraldehyde-3-phosphate dehydrogenase (Gapdh), ribosomal protein L27 (Rpl27), and acidic ribosomal phosphoprotein P0 (36B4) were used as reference genes. No significant difference in the housekeeping Ct values was observed between the two groups.

Table 2. Nucleotide sequence of primers used for RT-PCR.

Gene	GenBank accession no.	Forward primer	Reverse primer
Actb	NM_007393	5'AACCGTGAAAAGATGACCCAGAT	5'CACAGCCTGGATGGCTACGTA
Gapdh	NM_008084	5'ATCCTGCACCACCAACTGCTTA	5'CATCAGCCACAGCTTTCCAG
Rpl27	NM_011289	5'CGCCAAGCGATCCAAGATCAAGTCC	5'AGCTGGTCCCTGAACACATCCTTG
36B4	NM_007475	5'CTGAGTACACCTTCCCCTACTGA	5'CGACTCTTCTTTGCTTCAGCTTT
SR-A1	NM_031195	5'TTGAACAACATCACCAACGACCTC	5'AGTAAGCCCTCTGTCTCCCTTTTC
Cd36	NM_001159558	5'ATGGTAGAGATGGCCTTACTTGGG	5'AGATGTAGCCAGTGTATATGTAGGCTC
SR-B1	NM_016741	5'AAACAGGGAAGATCGAGCCAGTAG	5'CGTAGTGAAGAACCTGGGGCAT
Lep	NM_008493	5'TGACACCAAACCTCATCAAGACCA	5'AATGAAGTCCAAGCCAGTGACCCTC
LDLr	NM_010700	5'TGAGGTTCTGTCCATCTTCTTCCC	5'TTGATGTTCTTACGCCGCCAGTTC
VLDLr	NM_013703	5'TCAGAAGTCAGTGTCCCCCAAAGG	5'TGCCAATTCCTCCACATCAAGTAGCC
Stab-2	NM_138673	5'AACAACATTCCAGCCCTGATAAA	5'CTGCAAGGATGTCGCTAGCA

Statistical analysis

Statistical analysis was performed using Graphpad Prism software (GraphPad Software, La Jolla, California, USA). Results are depicted as means \pm SEM or individual data points with means \pm SEM. Student's two-tailed t-tests or a two-way ANOVA with a Bonferroni test for multiple comparisons were used to compare the data of two normally distributed groups. Welch's correction was used to correct for unequal variances and outliers were detected by a Grubbs' test. Spearman correlation coefficient was calculated using Prism software (GraphPad Software, La Jolla, California, USA). Probability value of $P < 0.05$ was considered statistical significant.

RESULTS

Previous findings by Brochériou et al. have suggested that the expression of Stab-1 is increased during atherosclerotic lesion development [13]. As evident from Figure 2A we also detected a higher gene expression of Stab-1 in diseased arteries as compared to non-atherosclerotic arteries. Upon induction of atherosclerotic lesion formation, the aortic expression of Stab-1 was markedly increased as compared to Stab-1 expression on baseline (270% increase, $p < 0.001$, figure 2A). Notably, after the initial macrophage infiltration phase (up to week 2), aortic Stab-

1 expression is reduced to a level that is still somewhat higher than that at baseline (figure 2A). These results were validated in an independent experiment under similar experimental conditions using RT-PCR to measure Stab-1 expression (data not shown). In accordance with the notion that macrophage Stab-1 expression is reduced during in vivo macrophage foam cell formation and lesion progression, exposure to the foam cell-inducing agent oxLDL decreases Stab-1 gene expression in BMDM (37% decrease, $p < 0.05$, figure 2B) and in PM (53% decrease, $p < 0.01$, figure 2C).

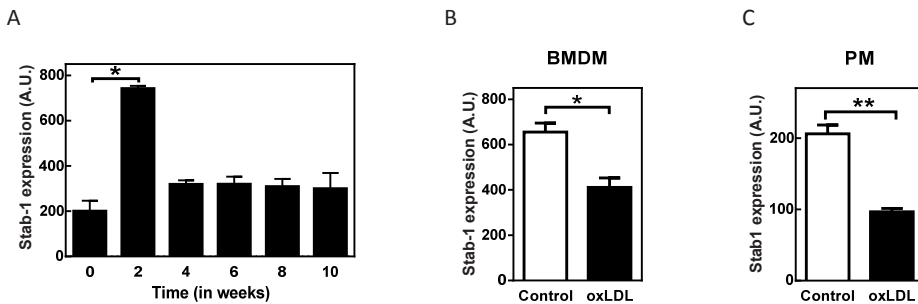


Figure 2. Expression of Stab-1 is modulated under atherogenic conditions. A) During initiation of atherosclerotic lesion in the first 2 weeks of lesion development, Stab-1 is increased as compared to baseline. During the progression of the lesion, Stab-1 values are normalized. B) Loading with oxidized LDL (oxLDL) reduced the relative gene expression of Stab-1 in bone marrow-derived macrophages (BMDM) and in thioglycolate-elicited peritoneal macrophages (PM;C). (N=3) Graphs represent means \pm SEM. * $P < 0.05$ ** $P < 0.01$

Bone marrow transplantation into hyperlipidemic mice is a well-established model to investigate the atherogenic potential of a macrophage-associated gene [22]. To uncover a potential contribution of macrophage Stab-1 to the pathogenesis of atherosclerosis, the effect of bone marrow-specific Stab-1 deletion on atherosclerotic lesion formation was investigated in LDLr KO mice on WTD. During the course of the experiment, the body weight was monitored regularly. Surprisingly, after the transient irradiation-induced drop in body weight, Stab-1 KO transplanted mice gained more weight as compared to WT transplanted mice (two-way ANOVA, $p < 0.001$, figure 3A). In parallel, the white adipocyte cell area was increased in adipose tissue of Stab-1 KO transplanted mice (43% increase, $p < 0.05$, figure 3B+C). White adipocyte cell area correlated significantly with body weight ($r = 0.82$, $p < 0.001$, figure 3D), indicating that this might be causal for the change in body weight. In further support of a more obese phenotype, the relative gene expression of the obesity-associated adipokine leptin was significantly increased in white adipose tissue of Stab-1 KO transplanted mice as compared to WT transplanted controls (124% increased, $p < 0.01$, figure 3E).

Despite the apparent difference in body weight development, plasma total cholesterol, free cholesterol and triglyceride levels were not significantly different between Stab-1 KO transplanted and control WT transplanted animals (figure 4A). The distribution of cholesterol

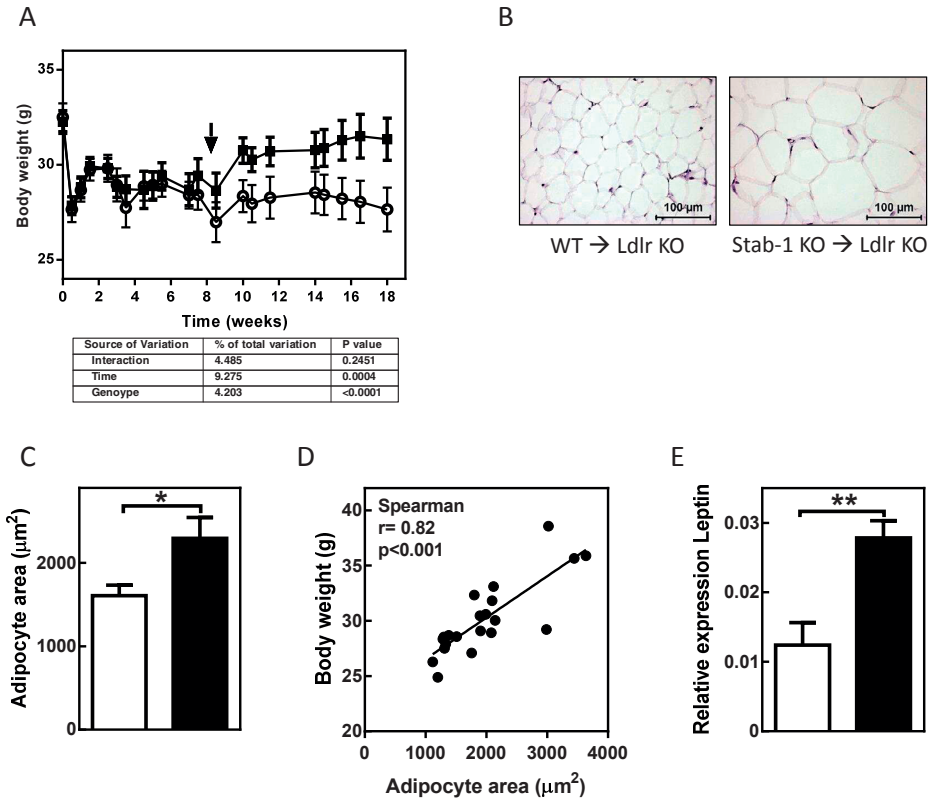


Figure 3. Total body weight is affected by bone marrow-specific Stab-1 deletion in LDLr KO mice as a result of changes in the white adipose tissue. A) Stab-1 KO transplanted LDLr KO mice (black squares; N=11) gained more weight as compared to WT transplanted control mice (white circles; N=12). Arrow indicates start Western-type diet feeding. B) Representative micrographs of white adipose tissue at magnification of 20x. C) Adipocyte cell area was significantly increased in Stab-1 KO transplanted mice (black bar; N=11) as compared to control WT transplanted mice (white bar; N=12). D) Body weight and adipocyte cell area correlated significantly. E) The relative expression of Leptin in white adipose tissue was significantly increased in Stab-1 KO transplanted mice (black bar; N=5) as compared to WT transplanted mice (white bar; N=6). Graphs represent means \pm SEM. * $P < 0.05$ ** $P < 0.01$.

over the different lipoprotein classes as measured with FPLC was also similar between both experimental groups (figure 4B).

Peritoneal leukocytes were isolated and the relative amount of macrophage foam cells was analyzed as a measure of in vivo foam cell formation. Despite the function of Stab-1 as a macrophage scavenger receptor for modified lipoproteins, bone marrow-specific Stab-1 deficiency was only associated with a trend towards a decrease in the extent of foam cell formation (41% decrease, $p = 0.07$, figure 5A+B). Real-time RT-PCR was used to identify possible compensatory changes in the expression of other receptors involved in macrophage lipoprotein uptake. Stabilin-2, a scavenger receptor showing 55% homology with Stab-1 on protein level, was not

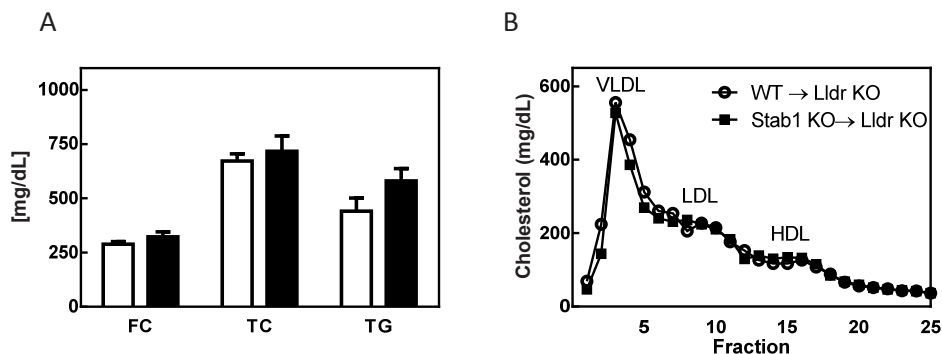


Figure 4. Plasma lipids are not changed after bone marrow-specific Stab-1 deletion in LDLr KO mice. A) The levels of total cholesterol or triglycerides were not different between the Stab-1 KO bone marrow transplanted group (black bars; N=11) and the WT transplanted group (white bars; N=12) after 9 weeks of Western-type diet feeding. B) The distribution of cholesterol over the lipoprotein fractions is not different in the Stab-1 KO transplanted group (black squares; N=3) as compared to the WT transplanted group (white circles; N=3). Graphs represent means \pm SEM.

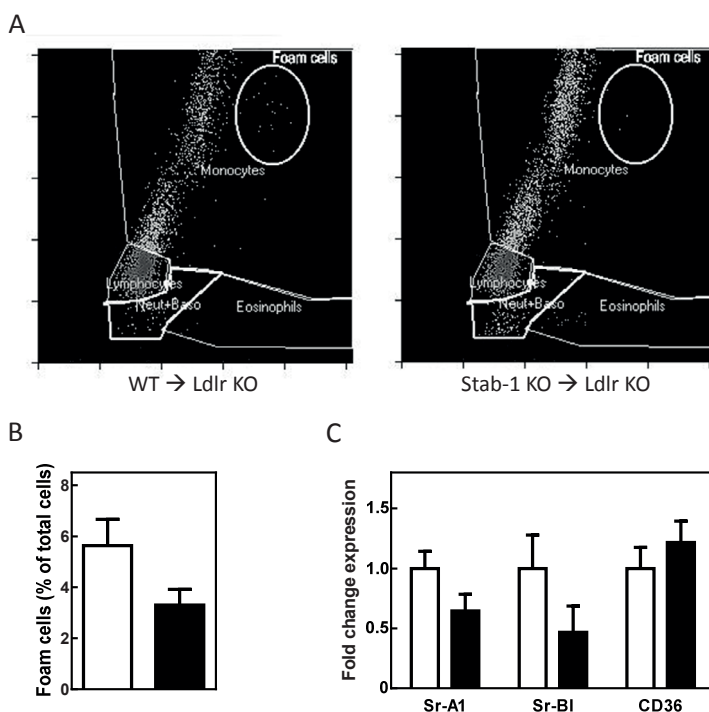


Figure 5. Bone marrow-specific Stab-1 deletion in LDLr KO mice does not affect in vivo foam cell formation. A) Representative scatterplots of the different leukocyte populations in the peritoneal cavity. The gate for foam cells is indicated with a circle. B) The percentage foam cells of the total peritoneal leukocyte population did not differ between Stab-1 KO transplanted (black bars; N=11) and WT transplanted mice (white bars; N=12). C) Fold change expression of scavenger receptors in the peritoneal leukocyte population (black bars; N=5) as compared to WT transplanted mice (white bars; N=6). Graphs represent means \pm SEM.

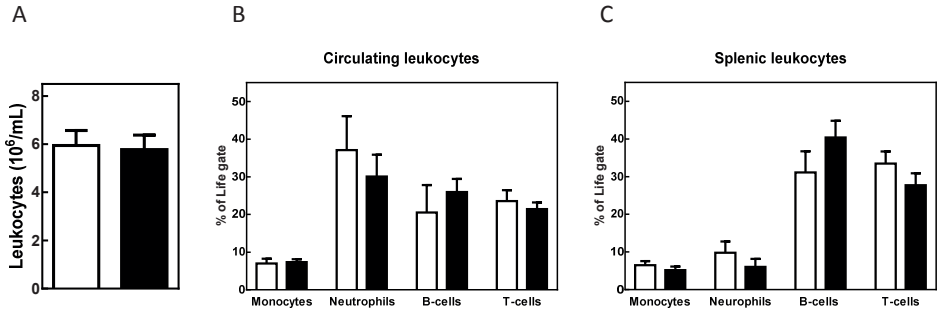


Figure 6. Total leukocyte number and distribution over leukocyte subpopulations is similar in Stab-1 KO and WT transplanted LDLr KO mice. A) Stab-1 KO transplanted mice (black bars; N=11) had similar total circulating leukocytes counts as WT transplanted mice (white bars; N=12). B) Bone marrow-specific deletion of Stab-1 (black bars; N=6) did not affect the contribution of the individual leukocyte subpopulations as compared to WT transplanted control mice (white bars; N=6) in the circulation or C) in the spleen. Graphs represent means \pm SEM.

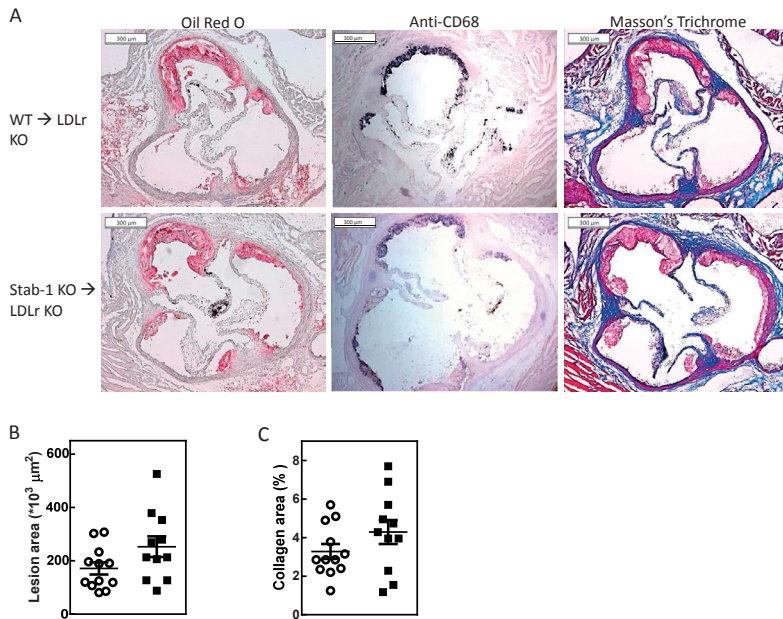


Figure 7. Bone marrow-specific Stab-1 deletion in LDLr KO mice did not affect atherosclerotic lesion size or composition. A) Representative micrographs of the aortic root stained with Oil Red O for neutral lipids (red), anti-CD68 for macrophages (black) and Masson's Trichrome for collagen (blue) did not show a difference in the lesion size or composition between Stab-1 KO transplanted mice. B) Atherosclerotic lesion area was not different in Stab-1 KO transplanted (black squares; N=11) and WT transplanted (white circles; N=12) LDLr KO mice after 9 weeks of WTD feeding. C) A similar percentage of collagen was measured in both Stab-1 KO transplanted (black squares; N=11) and WT transplanted (white circles; N=12) LDLr KO mice. Graphs represent means \pm SEM.

expressed at a level that could be reliably detected in either WT or Stab-1 KO peritoneal leukocyte fractions. LDLr and VLDLr gene expression was also virtually absent. The scavenger receptors SR-A1, SR-BI and CD36 were present but not significantly different between Stab-1 KO transplanted mice and WT transplanted controls (figure 5C).

Since monocyte (and endothelial) Stab-1 is implicated in the immune response [8,15], we measured the effect of bone marrow Stab-1 deficiency on circulating leukocytes. Total circulating leukocyte numbers were not significantly different between Stab-1 KO transplanted and WT transplanted mice (figure 6A). Moreover, there were no changes in the percentages monocytes, neutrophils, B-lymphocytes and T-lymphocytes in the circulation (figure 6B). Stab-1 KO transplanted mice also had a comparable splenocyte profile as WT transplanted control mice (figure 6C). The extent of atherosclerosis was determined in the aortic root. As evident from figure 7A, both groups of mice displayed significant lesion development after nine weeks of atherogenic WTD feeding. LDLr KO mice transplanted with WT bone marrow exhibited average aortic root lesions of $171 \pm 23 \times 10^3 \mu\text{m}^2$ that almost fully consisted of macrophages as judged from the CD68 staining (figure 7A). As can be appreciated from figures 7A and 7B, Stab-1 KO bone marrow transplanted mice also contained macrophage-rich early lesions that did not differ in size ($253 \pm 39 \times 10^3 \mu\text{m}^2$, $p=0.08$) as compared to WT transplanted mice. The amount of collagen, analyzed by Masson's Trichrome staining of the aortic root sections, was also similar in the Stab-1 KO transplanted and WT transplanted mice (figure 7A and 7C).

DISCUSSION

We aimed to uncover whether macrophage Stab-1 contributes to atherosclerotic lesion formation in mice. Here we show that bone marrow-specific deletion of Stab-1 did not translate into significant changes in the extent of in vivo foam cell formation. Furthermore, systemic lipid concentrations or circulating leukocytes were not altered as a result of the bone marrow transplantation. Consequently, Stab-1 KO transplanted mice displayed a similar atherosclerosis susceptibility as compared to WT transplanted mice.

Stabilin-2 (Stab-2) exhibits a 55% homology in protein sequence with Stab-1 [9]. Although the two receptors are related, the ligands of Stab-1 and Stab-2 are different. Whereas Stab-1 mostly binds modified lipoproteins and SPARC, the major ligands for Stab-2 include hyaluronan and AGE-modified proteins [4,23,24]. Schledzewski et al. showed that, despite the difference in ligands, both scavenger receptors are redundant as the individual single KO mice did not show major phenotypic changes while the double deficient mice died prematurely [25]. Hence, it cannot be excluded that absence of an effect of macrophage Stab-1 deficiency on atherosclerosis susceptibility might be nullified by the presence of functional Stab-2, especially since the presence of Stab-2 has also been shown in subsets of macrophages and murine atherosclerotic

lesions [26,27]. However important to note, we could not detect Stab-2 in macrophage foam cells in our in vitro experimental set-up. To further investigate the hypothesis of Stab-2 compensation for the loss of Stab-1 in macrophages, the functional presence of Stab-2 expressing macrophages in atherosclerotic lesions of Stab-1 KO transplanted mice needs to be established. Although endothelial progenitor cells can be derived from bone marrow, in our bone marrow transplantation atherosclerosis model we have never found any evidence of replacement of endothelial cells by cells from donor origin. However, Stab-1 and Stab-2 expression by liver sinusoidal endothelial cells may be able to compensate for Stab-1 deficiency in macrophages and may have distant effects on aortic atherosclerosis by controlling circulating ligands in the blood stream. It would therefore be valuable to compare the effects of Stab-1/Stab-2 single and double deficiency in total-body knockouts and in our bone marrow-specific model to investigate atherosclerotic lesion formation without the potentially confounding redundancy effects. Importantly, functional redundancy has also been shown for other macrophage scavenger receptors, i.e. SR-A1 and CD36. As such, the effects of deficiency of one or more scavenger receptors on atherosclerosis development in murine models is controversial and the conflicting outcomes are proposed to be dependent on the stage of the lesion development and the genetic make-up of the atherosclerotic background of the mice used for the experiment as reviewed by Moore and Freeman [28]. Here, we investigated Stab-1 deficiency in initial lesions specifically. During our in vitro foam cell experiments, we observed a downregulation of Stab-1 in foam cells of WT origin. Since Stab-1 is virtually absent in WT cells after foam cell induction, we do not expect any macrophage-specific Stab-1 effects on atherosclerotic lesion development in more advanced stages of the disease.

We observed an unexpected effect of bone marrow Stab-1 deficiency on body weight development. It is known that bone marrow-derived macrophages in adipose tissue play a key role in obesity [29,30]. Interestingly, the gene expression level of SPARC, a known ligand of Stab-1, in the adipose tissue is increased in mouse models for obesity [31] and in obese humans [32]. In addition, the level of SPARC in the serum of patients with type 2 diabetes is increased independent of obesity [33]. Based upon these combined findings, it can be proposed that the increased adiposity observed in Stab-1 KO transplanted mice is not a direct effect of macrophage Stab-1 deficiency but rather secondary to increased adipose tissue SPARC levels as a result of an inability of Stab-1 knockout macrophages in adipose tissue to clear SPARC. It would be interesting to measure SPARC levels in adipose tissue to further investigate this hypothesis.

In conclusion, we have shown that macrophage Stab-1 deficiency does not affect atherosclerosis susceptibility in LDLr KO mice. Notably, in addition to macrophages, Stab-1 is expressed in murine aortic endothelial cells as well as human coronary arterial endothelial cells [5,13]. Given that in response to pathogens and modified lipoproteins endothelial cells can acquire a type II (pro-inflammatory) activation state [34,35], future research in global and endothelial

cell-specific Stab-1 KO mice is warranted to potentially uncover a relevant contribution of endothelial Stab-1 in the pathogenesis of atherosclerosis.

ACKNOWLEDGEMENTS

We would like to thank P. van Santbrink and M.J. Kröner for their technical assistance during the experiments. Furthermore, we would like to thank I. Bot for providing the microarray data from the collar-induced lesion model for atherosclerosis. We acknowledge the support from the Netherlands CardioVascular Research Initiative: “the Dutch Heart Foundation, Dutch Federation of University Medical Centres, the Netherlands Organisation for Health Research and Development and the Royal Netherlands Academy of Sciences” for the GENIUS project “Generating the best evidence-based pharmaceutical targets for atherosclerosis” (CVON2011-19 to M.van Eck). This study was supported by the Netherlands Organization for Scientific Research (VICI Grant 91813603 to M. van Eck) and Dutch Heart Foundation grant 2012T080 awarded to M. Hoekstra; M. van Eck is an Established Investigator of the Netherlands Heart Foundation (Grant 2007T056).

REFERENCES

- [1] Van Berkel, T.J.C., Out, R., Hoekstra, M., Kuiper, J., Biessen, E., Van Eck, M., 2005. Scavenger receptors: Friend or foe in atherosclerosis? *Current Opinion in Lipidology* 16(5): 525–35, Doi: 10.1097/01.mol.0000183943.20277.26.
- [2] Goerdt, S., Walsh, L.J., Murphy, G.F., Pober, J.S., 1991. Identification of a novel high molecular weight protein preferentially expressed by sinusoidal endothelial cells in normal human tissues. *The Journal of Cell Biology* 113(6): 1425–37.
- [3] Li, R., Oteiza, A., Sørensen, K.K., Mccourt, P., Olsen, R., Smedsrød, B., et al., 2011. Role of liver sinusoidal endothelial cells and stabilins in elimination of oxidized low-density lipoproteins (33): 71–81, Doi: 10.1152/ajpgi.00215.2010.
- [4] Kzhyshkowska, J., Workman, G., Cardo-Vila, M., Arap, W., Pasqualini, R., Gratchev, A., et al., 2006. Novel Function of Alternatively Activated Macrophages: Stabilin-1-Mediated Clearance of SPARC. *The Journal of Immunology* 176(10): 5825–32, Doi: 10.4049/jimmunol.176.10.5825.
- [5] Adachi, H., Tsujimoto, M., 2002. FEEL-1, a novel scavenger receptor with in vitro bacteria-binding and angiogenesis-modulating activities. *Journal of Biological Chemistry* 277(37): 34264–70, Doi: 10.1074/jbc.M204277200.
- [6] Park, S.-Y., Jung, M.-Y., Lee, S.-J., Kang, K.-B., Gratchev, A., Riabov, V., et al., 2009. Stabilin-1 mediates phosphatidylserine-dependent clearance of cell corpses in alternatively activated macrophages. *Journal of Cell Science* 122(18): 3365–73, Doi: 10.1242/jcs.049569.
- [7] Tamura, Y., Adachi, H., Osuga, J., Ohashi, K., Yahagi, N., Sekiya, M., et al., 2003. FEEL-1 and FEEL-2 are endocytic receptors for advanced glycation end products. *The Journal of Biological Chemistry* 278(15): 12613–7, Doi: 10.1074/jbc.M210211200.
- [8] Karikoski, M., Irjala, H., Maksimow, M., Miiluniemi, M., Granfors, K., Hernesniemi, S., et al., 2009. Clever-1/Stabilin-1 regulates lymphocyte migration within lymphatics and leukocyte entrance to sites of inflammation. *European Journal of Immunology* 39: 3477–87, Doi: 10.1002/eji.200939896.
- [9] Adachi, H., Tsujimoto, M., 2002. FEEL-1, a novel scavenger receptor with in vitro bacteria-binding and angiogenesis-modulating activities. *The Journal of Biological Chemistry* 277(37): 34264–70, Doi: 10.1074/jbc.M204277200.
- [10] Rantakari, P., Patten, D.A., Valtonen, J., Karikoski, M., Gerke, H., Dawes, H., et al., 2016. Stabilin-1 expression defines a subset of macrophages that mediate tissue homeostasis and prevent fibrosis in chronic liver injury. *Proceedings of the National Academy of Sciences* 113(33): 9298–303, Doi: 10.1073/pnas.1604780113.
- [11] Palani, S., Maksimow, M., Miiluniemi, M., Auvinen, K., Jalkanen, S., Salmi, M., 2011. Stabilin-1/CLEVER-1, a type 2 macrophage marker, is an adhesion and scavenging molecule on human placental macrophages. *European Journal of Immunology* 41(7): 2052–63, Doi: 10.1002/eji.201041376.
- [12] Goerdt, S., Bhardwaj, R., Sorg, C., 1993. Inducible expression of MS-1 high-molecular-weight protein by endothelial cells of continuous origin and by dendritic cells/macrophages in vivo and in vitro. *The American Journal of Pathology* 142(5): 1409–22.
- [13] Brochériou, I., Maouche, S., Durand, H., Braunersreuther, V., Le Naour, G., Gratchev, A., et al., 2011. Antagonistic regulation of macrophage phenotype by M-CSF and GM-CSF: Implication in atherosclerosis. *Atherosclerosis* 214(2): 316–24, Doi: 10.1016/j.atherosclerosis.2010.11.023.

- [14] Mosig, S., Rennert, K., Krause, S., Kzhyshkowska, J., Neunubel, K., Heller, R., et al., 2009. Different functions of monocyte subsets in familial hypercholesterolemia: potential function of CD14+CD16+ monocytes in detoxification of oxidized LDL. *The FASEB Journal* 23(3): 866–74, Doi: 10.1096/fj.08-118240.
- [15] Palani, S., Elima, K., Ekholm, E., Jalkanen, S., Salmi, M., 2016. Monocyte Stabilin-1 Suppresses the Activation of Th1 Lymphocytes. *Journal of Immunology* 196(1): 115–23, Doi: 10.4049/jimmunol.1500257.
- [16] Chu, E.M., Tai, D.C., Beer, J.L., Hill, J.S., 2013. Macrophage heterogeneity and cholesterol homeostasis: Classically-activated macrophages are associated with reduced cholesterol accumulation following treatment with oxidized LDL. *Biochimica et Biophysica Acta - Molecular and Cell Biology of Lipids* 1831(2): 378–86, Doi: 10.1016/j.bbalip.2012.10.009.
- [17] Oh, J., Riek, A.E., Weng, S., Petty, M., Kim, D., Colonna, M., et al., 2012. Endoplasmic reticulum stress controls M2 macrophage differentiation and foam cell formation. *Journal of Biological Chemistry* 287(15): 11629–41, Doi: 10.1074/jbc.M111.338673.
- [18] Ackers-johnson, M., Talasila, A., Sage, A.P., Long, X., Bot, I., Morrell, N.W., et al., 2015. Myocardin Regulates Vascular Smooth Muscle Cell Inflammatory Activation and Disease. *Arterioscler Thromb Vasc Biol.* 35(4): 817–28, Doi: 10.1161/ATVBAHA.114.305218.Myocardin.
- [19] Thüsen, J.H. Von Der, Berkel, T.J.C. Van., Biessen, E.A.L., 2001. Induction of Rapid Atherogenesis by Perivascular Carotid Collar Placement in Apolipoprotein E – Deficient and Low-Density Lipoprotein Receptor – Deficient Mice. *Circulation*: 1164–71.
- [20] Out, R., Hoekstra, M., Hildebrand, R.B., Kruit, J.K., Meurs, I., Li, Z., et al., 2006. Macrophage ABCG1 Deletion Disrupts Lipid Homeostasis in Alveolar Macrophages and Moderately Influences Atherosclerotic Lesion Development in LDL Receptor-Deficient Mice. *Arteriosclerosis, Thrombosis, and Vascular Biology* 26(10): 2295 LP-2300.
- [21] Chomczynski, P., Sacchi, N., 1987. Single-Step Method of RNA Isolation by Acid Guanidinium Extraction. *Analytical Biochemistry* 162: 156–9.
- [22] Schiller, N.K., Kubo, N., Boisvert, W.A., Curtiss, L.K., 2001. Effect of γ -Irradiation and Bone Marrow Transplantation on Atherosclerosis in LDL Receptor – Deficient Mice. *Arteriosclerosis, Thrombosis, and Vascular Biology (Ldl)*: 1674–81.
- [23] Kzhyshkowska, J., Gratchev, A., Brundiens, H., Mamidi, S., Krusell, L., Goerdts, S., 2005. Phosphatidylinositol 3-kinase activity is required for stabilin-1-mediated endosomal transport of acLDL. *Immunobiology* 210(2–4): 161–73, Doi: 10.1016/j.imbio.2005.05.022.
- [24] Hansen, B., Longati, P., Elvevold, K., Nedredal, G.-I.L., Schledzewski, K., Olsen, R., et al., 2005. Stabilin-1 and stabilin-2 are both directed into the early endocytic pathway in hepatic sinusoidal endothelium via interactions with clathrin/AP-2, independent of ligand binding. *Exp Cell Res* 303(1): 160–73, Doi: 10.1016/j.yexcr.2004.09.017.
- [25] Schledzewski, K., Géraud, C., Arnold, B., Wang, S., Gröne, H., Kempf, T., et al., 2011. Deficiency of liver sinusoidal scavenger receptors stabilin-1 and -2 in mice causes glomerulofibrotic nephropathy via impaired hepatic clearance of noxious blood factors. *J Clin Invest.* 121(2), Doi: 10.1172/JCI44740. nodes.
- [26] Lee, G.Y., Kim, J.H., Oh, G.T., Lee, B.H., Kwon, I.C., Kim, I.S., 2011. Molecular targeting of atherosclerotic plaques by a stabilin-2-specific peptide ligand. *Journal of Controlled Release* 155(2): 211–7, Doi: 10.1016/j.jconrel.2011.07.010.